26th EPS Conf. on Contr. Fusion and Plasma Physics, Maastricht, 14 - 18 June 1999 ECA Vol.23J (1999) 285 - 288

Transport Barriers in Optimized Shear Toroidal Confinement

W. Horton[1], P. Zhu[1], T. Tajima[1], Y. Kishimoto[2],
J.–M. Kwon[3], D.–I. Choi[3]
[1]*Institute for Fusion Studies, Univ. of Texas, Austin, TX 78712*
[2]*Naka Fusion Res. Establishment, JAERI, Naka, Ibaraki 310–0195 Japan*
[3]*Dept. of Physics, KAIST, Taejon 305–701, KOREA*

Abstract

The turbulent transport properties in low magnetic shear toroidal confinement systems are reported and compared with those in reversed magnetic shear (RS). The basic properties of RS systems are (1) the breaking of the ballooning mode symmetry with a new local mirror symmetry in its place and (2) the introduction of shearless invariant curves in the guiding center phase space. For low shear the density of the drift wave mode rational surfaces is sufficiently low to reduce the toroidal coupling leaving the cylindrical drift wave turbulence. We find that the optimized shear (OS) confinement barriers are explained by the Hamaguchi–Horton E_r–shearing parameter rather than the Hahm–Burrell parameter. For a JET internal transport barrier discharge identified for the coordinate workshop analysis we compare the r,t–development of the two E_r–shearing parameters with onset and radial expansion of the internal transport barrier (ITB).

1 Introduction

The turbulent transport properties of tokamak plasmas are strongly controlled by the magnetic shear and the radial electric field shear. Both types of shear control transport by influencing the spatial structure of the fluctuations. The magnetic shear $s = rq'/q$ controls the density of mode rational surfaces [1], the radial width w_k of the modes localized to the mode rational surfaces $m = nq(r_{m,n})$. The radial electric field shear controls the tilting of the mode structures in the poloidal cross–section and shifts the centers of the modes off the mode rational surfaces by $\Delta x_0 = -\mathcal{E}/(2s^2\gamma_s^2)$, where $\mathcal{E} = (\mathbf{k}\cdot\mathbf{u})'/\omega_k$ and $\gamma_s = c_s/qR\omega_k$. The shifted position of the mode is determined by minimizing the local radial wavenumber $k_r^2 = Q(\omega, m, n, r)$ in the presence of the magnetic shear $k_{||} = (m - nq(r))/qR$ and E_r–shear $\mathcal{E} = \frac{\partial}{\partial r}(E_r/RB_p)$ [2]. The fastest linear growth occurs for modes with the minimum k_r^2 consistent with the sheared equilibrium profiles. The growth rates are reduced by the second order shift in the drift wave eigenvalues $\Delta\lambda = \mathcal{E}\Delta x = (\mathcal{E}/s\gamma_s)^2$. In this manner one derives the dimensionless shear–flow transport parameters

$$\Upsilon_s = \left|\frac{qR}{c_s s}\frac{dv_E}{dr}\right| \simeq \sqrt{\frac{m_i}{T_e}}\left|\frac{R\partial_r(E_r/RB_\theta)}{\partial_r \ln q}\right| \qquad (1)$$

that controls the reduction of transport with increased E_r–shear and/or weak magnetic shear. For reference, the Hahm–Burrell shearing parameter is

$$\omega_s \simeq \left| \frac{RB_p}{B_T} \frac{d}{dr} \left(\frac{E_r}{RB_p} \right) \right| \tag{2}$$

and arises from rate of decay of the two–point decorrelation in ambient turbulence. The shear–shear stability/transport parameter is also encountered in Waelbroeck [3]. This dimensionless parameter appears to be a sensitive indicator of the onset of enhanced confinement as shown in the comparison of the reversed shear (RS) and enhanced reversed shear (ERS) discharges in TFTR [4]. Here we investigate the optimized shear discharges in JET with respect to this stability/transport parameter.

2 Results

In Fig. 1, we show the $q(r)$–profile and the power balance $\chi_i^{\rm BP}$ for $t = t_1$ for the optimized shear (OS) discharge JET 40542. In OS discharges the central shear is weak and the edge shear is strong characteristic of current profiles with a large bootstrap fraction. The density of rational surfaces for the toroidal mode $n = 20$ is shown in Fig. 2 for constant mode width ($w_k/a = 0.01$) and amplitude for simplicity. The central modes have only weak radial overlap, while the region beyond $\rho > 0.7$ has strong mode overlapping. The number of overlapping modes is given by the number of the dark bands. Immediately, we see that the local value of the Chirikov overlap parameter K for the drift wave map description increase strongly toward the edge. In the core the overlap is weak and as the $q(r)$ profile develops a minimum the drift wave guiding center map changes from the 1 parameter (K) standard map to the 2 parameter nontwist map. For the ion guiding centers the rotation of the wave–particle phase is determined both by the q–profile and the E_r–profile while for electron transport it is the q–profile that dominates the phase changes.

The radial electric field in the laboratory frame is dominated by the motional electromotive force $E_r \simeq u_\phi B_p$ due to the use of all co–injection in the JET optimized shear discharges. We calculate the electric field in the rotating frame $E_r - u_\phi B_p$ using neoclassical theory for deuterium–carbon plasma for arbitrary impurity parameter $\alpha = Z_x^2 n_x/n_i$ by inverting the full (6×6) friction–viscosity matrices [4]. For one of the coordinated data analysis discharges the results are shown in Fig. 3. The field is very large ($E_{\rm max} \sim 140\,{\rm kV/m}$) and peaked in the steep pressure gradient zone. This zone is also the region of suppressed ion transport shown in Fig. 1.

From the electric field the Hahm–Burrell shearing frequency ω_s and the shear–shear parameter are computed and shown in Fig. 3. Due to the maximum of E_r/RB_θ, both parameters vanish near $\rho = 0.9$. The shear–shear parameter is greater than 1.0 in regions $\rho = [0.05, 0.2]$ and [0.4, 0.7] where 2 is the value found in the 3D slab simulation for strong suppression of the turbulent ITG thermal diffusivity. The ratio $\omega_s/\gamma^{\rm ITG}$, where $\gamma^{\rm ITG} = c_s/(L_{T_i}R)^{1/2}$, is relatively constant ($\lesssim 0.3$) for $\rho \leq 0.9$.
To explore further the correlation of the shear–shear parameter with enhanced confinement we plot the time evolution of Υ_s in Fig. 4 compared with the total stored energy W_{tot} and its confinment time τ_E, along the ITER–97 L mode scaling for τ_E. In addition we show the ratio of the Hahm–Burrell shearing rate over the ITG mode growth rate $\omega_s/\gamma^{\rm ITG}$ changing with time. Again the shear–shear parameter Υ_s appears to show a clearer correlation with improved confinement. Parail *et al.* [5] find a similar result from interpretive simulations.

3 Conclusion

We have analyzed the optimized shear discharges of the coordinated data analysis program for JET with respect to the roles of magnetic shear and E_r–shearing on the transport. The stability/transport parameter in Eq. (1) that describes the shift in the drift wave eigenvalues from the E_r–shear induced shifting and tilting of the fluctuation spectrum gives a good indicator of the enhanced confinement. The features of the Υ_s parameter that forecasts improved confinement are (1) increasing E_r–shear; (2) weaker magnetic shear and (3) higher working gas ion mass. Future work using these results in a predictive transport code will help clarify the ability of the shear–shear parameter to forecast and quantify improved confinement regimes.

References

[1] A.D. Beklemishev and W. Horton, Phys. Fluids B **4**, 2176 (1992).

[2] S. Hamaguchi and W. Horton, Phys. Fluids B **4**, 319 (1992).

[3] F.L. Waelbroeck, *et al.*, Phys. Fluids B 4, 2441 (1992).

[4] P. Zhu, W. Horton, and H. Sugama, Phys. Plasmas, **6** 2503 (1999).

[5] V.V. Parail, *et al.*, Nucl. Fusion **39**, 429 (1999).

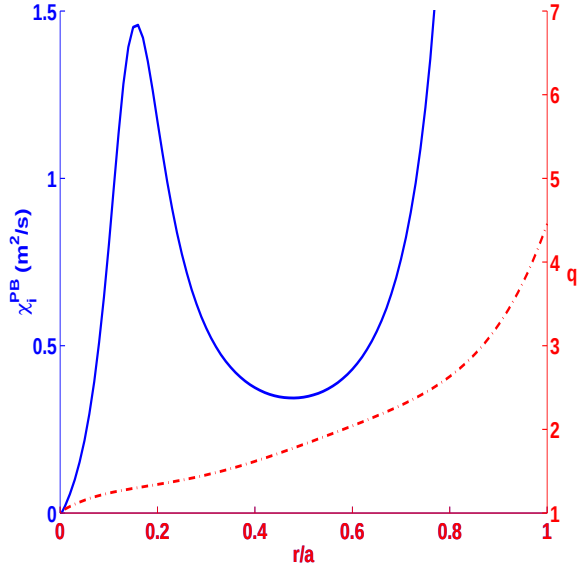

Figure 1: The power balance ion thermal diffusivity and the q–profile near time of maximum transport barrier.

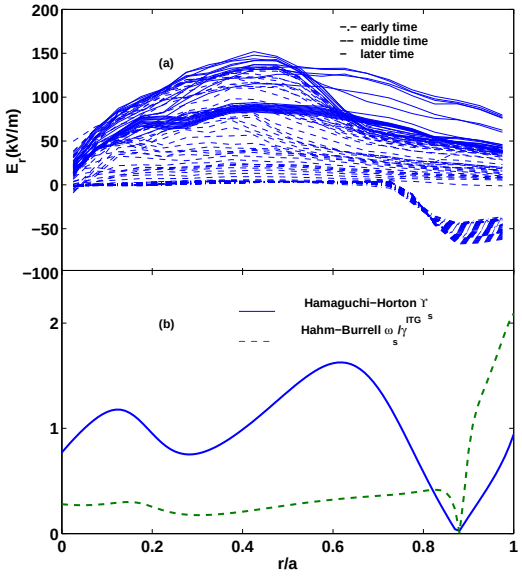

Figure 3: (a) The E_r–profiles for all times through the pulse and (b) the dimensionless shear rates $\omega_s/\gamma^{\rm ITG}$ and Υ_s in Eq. (1).

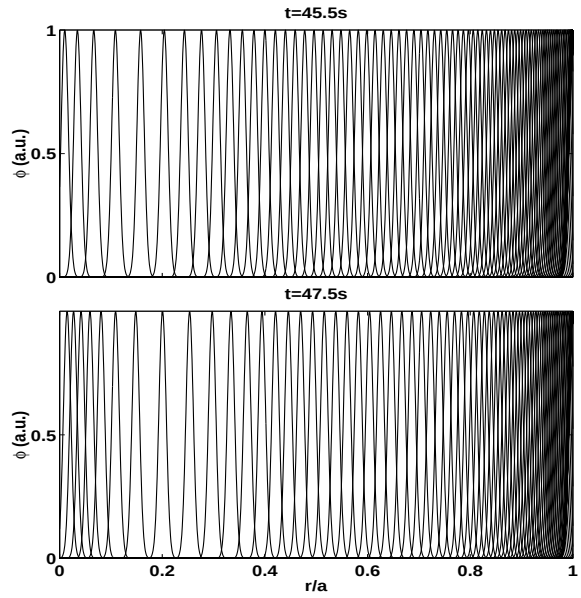

Figure 2: Overlapped drift wave profiles localized at mode rational surfaces for $n = 20$ ($k_y\rho_s \simeq 0.3$) shift with time.

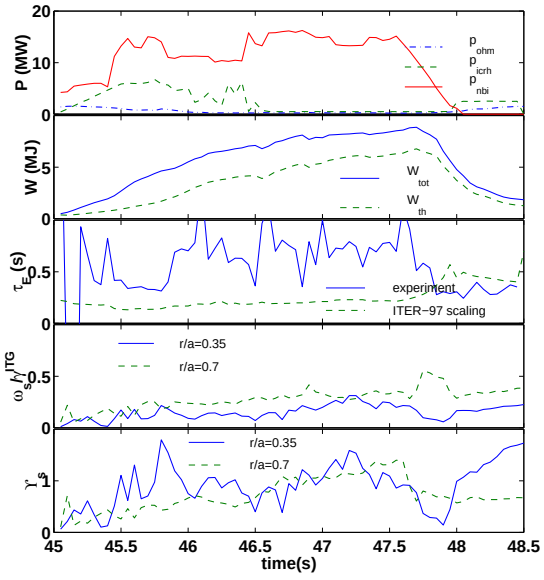

Figure 4: The correlation between the improved confinement (W_{tot}, τ_E) and shearing rates $\omega_s/\gamma^{\rm ITG}$ and Υ_s in JET shot# 40542.